Monim H. Al-JIBOORI, Sundus H. JABER

College of Science, Mustansiriyah University, Baghdad, Iraq

Characteristics of C_μ^2 derived from ultrasonic anemometer in an urban boundary layer

Introduction

The development of optical communication systems is recently considered for a variety of applications, particularly within the last mile access networks. Free space optical (FSO) technology is commonly used in urban and mountainous areas, because of the complexity associated with setting up the technique of fiber optics. For better performance rate in operating FSO systems, it is required a direct line of sight free of atmospheric phenomena such as rain, fog, dust and turbulence (Henniger & Wilfert, 2010).

In this paper, turbulence effect will be involved, because of its availability in the atmosphere caused by variation in temperature and wind, which leads to spatial and temporal random fluctuations of the refractive index along the beam propagation through the channel. This effect primarily causes phase shifts of the propagating optical signals resulting distortions of the quality of the received image. The most significant parameter that is used in expressing optical turbulence is refractive index structure function coefficient (C_μ^2) which is a function of position, time and height. When a light beam propagates through such a turbulent medium its interaction with the eddies produces random variations in the amplitude and phase of the signal (Ishimaru, 1997; Altowij, Alkholidi & Habib, 2010). These variations in the refractive index of the Earth's atmosphere are responsible for random fluctuations in the signal carrying laser beam intensity called scintillations.

The most studies published in the literature have been primarily concerned with the development of an atmospheric turbulence theory and its effect on the performance of optical system. Zku & Kahn (2002) designed an experiment to simulate FSO communication through

atmospheric turbulence channels. Mathematical models also used to study the influence of scintillation on optical wireless propagation such as Romain, Larkin, Ghavel, Paulson and Nykolak (2001) and Prokeš (2009). However, observationally diurnal and seasonal variations of C_μ^2 at several heights within the surface boundary layer were carried out by Wesely and Alcaraz (1973) and Walters, Kunket and Hoidale (1981), in which abroad maximum was around mid-day, while two minima were near sunrise and sunset. Later Roadcap and Tracy (2009) made measurements of C_μ^2 during day and night times from the surface to 10 km for different boundary layers: dry convective, moist convective and marine inversion. They found that C_μ^2 was higher through the convective layer. In above papers mean slow data were used to drive this parameter, while in this work fast-response data measured by ultrasonic anemometer are employed to calculate C_μ^2.

The purpose of this paper is to calculate C_μ^2 and then study its characteristics in the urban boundary layer such as Baghdad city. This will imply presenting diurnal and seasonal variation of C_μ^2. The relation between this coefficient and stability parameter will be also examined. Lastly evaluation of the effect of both rain and fog on C_μ^2 will be presented.

Theoretical concepts

Understanding of atmospheric turbulence is based on the Kolmogorov–Obukhov theory, which allows the computation of statistical quantities in a turbulent system. The applicability of their theory is in the range, called as iner-

tial sub-range, within the inner and outer scale sizes. In this range, the fluctuations of the turbulent quantitiestend to have independent properties and universal behavior. Consequently, turbulent flows of interest are isotropic.

Tatarski applied this inertial sub--range concept to the effects of atmospheric turbulence on electromagnetic radiation, solving the wave equation by employing the Rytove approximation (Panofsky & Dutton, 1984), i.e. expressing the wave equation in terms of the logarithm of the amplitude and then applying a perturbation technique. With comprehensive analysis, Tatarski arrived at an expression for the wave structure function, $D(p)$ (Fried, 1965). Its importance to atmospheric turbulence lies in ability to represent all the statistics of phase and amplitude fluctuations of a propagated wave, and it therefore contains information concerning the shape of the deformed wave front. By definition, for infinite plane wave and horizontal propagation paths, Tatarski concluded that

$$D(p) = 2.91 \, k_\lambda^2 \, p_s^{5/3} \int_0^L C_\mu^2(s) ds \qquad (1)$$

where:
k_λ – wavenumber equal $2\pi\lambda^{-1}$ with λ is wavelength);
C_μ – is the refractive index structure coefficient representing the (optical) strength of the turbulence;
s – position along the propagation path;
p_s – sample point separation in the aperture plane equal $\lambda X_L f_s$;
f_s – spatial frequency in the image plane (cycles per unit length);
X_L – local length of the lens.

Also he derived the $D(p)$ for the propagation of a spherical wave over a horizontal path, i.e.

$$D(p) = 2.91\, k_\lambda^2 p_s^{5/3} \int_0^L C_\mu^2(s) \left(\frac{s}{L}\right)^{5/3} ds$$

(2)

We notice that both Eqs. (1) and (2) depend on the propagation path length, the wavelength, the strength of the turbulence along the path and the nature of the unperturbed wave front (Hulett, 1967).

Optical turbulence

As shown in the previous section, the optical strength of turbulence can be represented as C_μ. There is considerable evidence (both experimental and theoretical) to suggest that, in the inertial sub-range (Fried, 1965)

$$C_\mu^2 = D_\mu(p)\, p_s^{-2/3}$$

(3)

where:
$D_\mu(p)$ – refractive index structure function defined as

$$D_\mu(p) = \overline{\left[\Delta\mu(x + p_s) - \Delta\mu(x)\right]^2}$$

(4)

where:
x – point in the path of the propagated wave.

The C_μ^2, through its dependence on the vertical temperature gradient, shows a complete dependence on the time of day, season, terrain, height and meteorological conditions (Hagelin, Masciadri & Lascaux, 2005).

Optical turbulence (OT) is formed by the wind shear and the thermally stable layer of atmosphere. The vertical distribution of the OT is described by the structure function C_μ^2. The most intense OT is found near the surface, and second weaker maximum can be found near the jet stream at ~12 km above sea level (Canuet, 2014).

Calculation of C_μ^2

Using local temperature scaling data (T_{*1}), which is constant for any given atmospheric conditions regardless of the sensor's height, and represents the local vertical temperature gradient. C_μ^2 can be calculated by Tatarski method (Fried, 1965).

$$C_\mu = 2.40 \kappa^{2/3} h^{-1/3} 10^{-6} T_{*l}$$

(5)

where:
κ – von Kármán constant of value equal ~ 0.4;
h – height above ground level;
T_{*l} can be calculated as follows:

$$T_{*l} = -\frac{\overline{(w'T')}_l}{u_{*l}}$$

(6)

where:
T' – temperature fluctuations calculated as $T' = T - \overline{T}$ with T is the observed temperature and $\overline{T}$ is the mean temperature;
u_{*l} = local friction velocity calculated as follow:

$$u_{*l} = \sqrt{\left|\overline{-u'w'}\right|}$$

(7)

where:
u', w' are the fluctuations of longitude and vertical components of wind.

The subscript 'l' denotes 'local', so all the variables in Eqs. 5, 6 and 7 are determined locally.

Site description and measured data

The instrument used to achieve this work is 3D ultrasonic anemometer mounted on the roof of atmospheric science building (ASB), College of Science, Mustansiriya University located at northeast of Baghdad as shown in Figure 1. The height of the device is 19 m above the ground. The university consists of big buildings especially those located to the south and the east. The area of university campus is 28,000 m^2 and surrounded with houses, shops, one bridge and scattered parks.

FIGURE 1. Ultrasonic anemometer installed on ASB

Fast-response data of three wind speed components (u, v, w) and temperature made by Gill Sonic and have the operation of wind master pro (1561-pk--020/W+ option) for it three axes ultrasonic anemometer, with no moving parts. The units of wind speed, output rate and formats are all users selectable and wind master pro constructed from marine grade stainless steel 316 mm, which can perform measurements in average wind speed up to 65 m·s^{-1}.

The measurements from device were programmed to monitor one for each second means 1 Hz. The recorded data at random days were taken on CD to calculate C_μ^2 as a single level. Unfortunately, the observing periods for these data are not continuous, and irregular, but they have interval 15 days with total number of 290 runs, as reported in Table 1 for more details. The clear sky days and the certain weather situations were involved through these days. To obtain the data more stationary, a few data at beginning and ending of each run are removed.

After finding the values of C_μ^2, the Excel program for making statistical analysis and the Origin software 9.2 for drawing plots were used in the present paper.

TABLE 1. The dates, periods and no. of daily runs for turbulence instrument data

Date of observation	Season	Period [day]	No of runs	Weather status
6, 13, 27, 28 Dec. 2015, 3 June 2016	winter	5	80	rain
11, 25, 26 April 2016	spring	3	42	fog
1, 2, 3, 4, 5, 6, 7 July 2016	summer	7	168	clear sky
Total sum		15	290	

Results and discussion

Diurnal variations of C_μ^2

The ultrasonic anemometer observation as a quick-response device for measuring wind speed components in m·s^{-1} and the temperatures in °C, that were converted to Kelvin scale, were used to find T_{*l} and u_{*l} values from Eq. (6) and (7), respectively. Values of T_{*l} are substituted in Eq. (5) to find the values of C_μ using the height representing the height of the device (19 m). These values were double as required in Eqs. (1) and (2), and can make also a comparison them to other common literatures as reported in Table 1. Double values of $C_\mu(C_\mu^2)$ for each hour during every day were hourly averaged for the period of the study. The mean hourly values of C_μ^2 for three seasons: winter, spring and summer, were calculated. For avoiding frequencies when discussion significant C_μ^2 results in this paper, all their values are multiplied by power factor 10^{-18}. Generally, the values of C_μ^2 are the lowest in winter compared to other seasons.

Figure 2 shows the variations of mean hourly C_μ^2 during winter except from 1:00 to 8:00 due to the lack of data and the reason was the power outage during that period. In general, high variation of C_μ^2 is clear during day hours even though these values are averages. This belongs to the fact that the different weather situations (224) are more frequent during this season as shown in Table 1. The mean values of C_μ^2 across the whole day appear highly fluctuating, but gradually begin to rise until it reached its highest value at 16 where its value is 8,000 m$^{-2/3}$ and that the lowest value is at 23:00 where the value of C_μ^2 at that hour is 5.5 m$^{-2/3}$. The interesting feature in this figure is the absence of turbulent motions at night time, which appear to has lowest values of C_μ^2 and probably approach to zero.

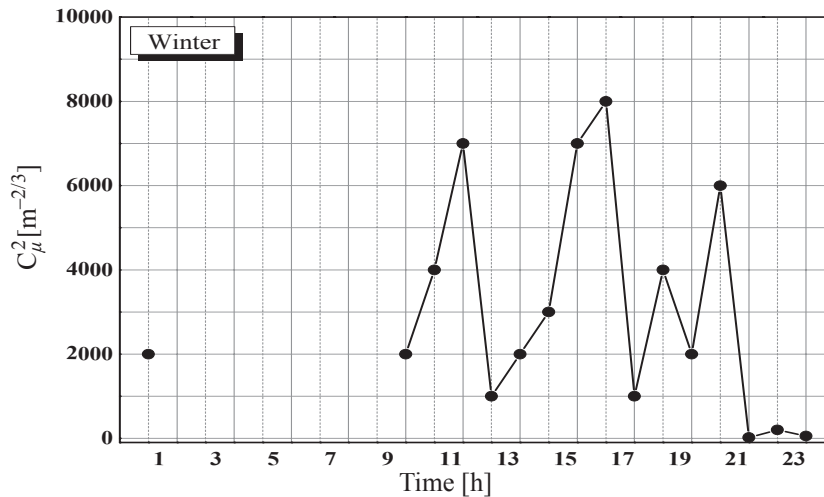Figure 3 shows hourly means of C_μ^2 for data available in spring (see Table 1).

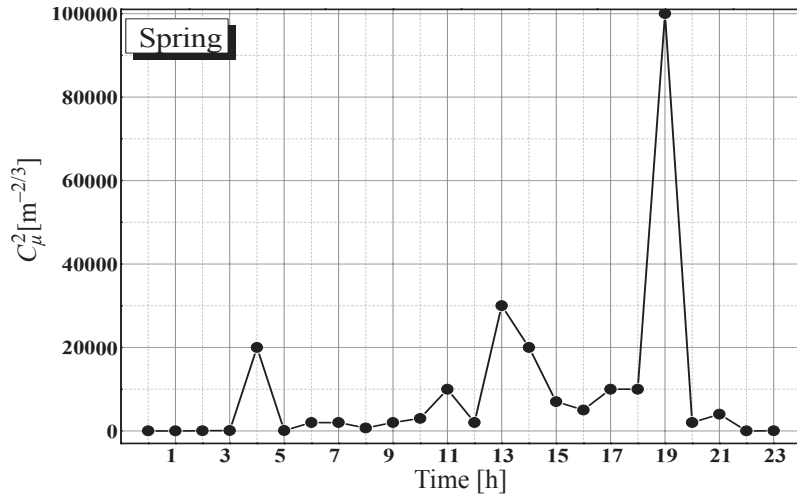FIGURE 2. Diurnal variation of mean C$_\mu^2$ values during all day in winter

FIGURE 3. Diurnal variation of mean C_μ^2 values during all day in spring

They have relatively large values corresponding to winter and much less values respect to summer as will be shown in next discussion. Highest effect of optical turbulence is found after sunset at 19:00 pm with value $10^5 m^{-2/3}$. There is gradual increase in the C_μ^2 values at day time such as from sunrise to sunset time. In contrast, these values decrease sharply to be lowest at dark night approaching to about less than 1 $m^{-2/3}$.

In summer, the highest values of C_μ^2 are fairly especially at 13:00 which its value about $5 \cdot 10^6 m^{-2/3}$ and lowest value occurs at midnight with $2 \cdot 10^4 m^{-2/3}$, as illustrated in Figure 4. The latter value is larger than that at maximum value at winter. In Iraq this season has extreme
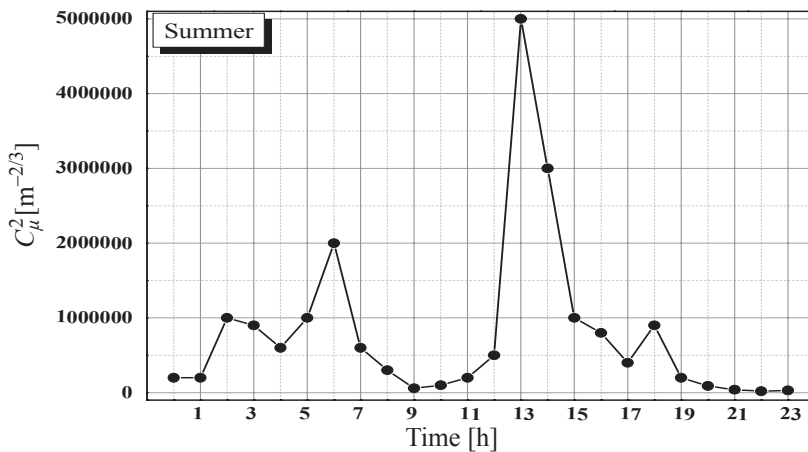

FIGURE 4. Diurnal variation of mean C_μ^2 values during all day in summer

values of air temperature exceeds 45°C. The significant effect of atmospheric turbulence appears clearly at summer with biggest values during the whole year. It is noted that there is large range of C_μ^2 values during the whole day, as shown in Figure 4.

As shown from the above discussions, the influence of atmospheric turbulence on the propagation of optical communications will be observed at noon time, where the sun is at its maximum activity, especially at summer season. This means the signal power received by receiving instrument will be affected and then to be weaken.

The effect of atmospheric stability on C_μ^2

In this subsection, an attempt to study the relation between refractive index structure coefficient and atmospheric stability through the different seasons, because as shown in previous sub-section, there was large variations in C_μ^2 values during these seasons.

Using fast-response data, local Monin–Obukhov length (Λ) was determined after calculating u_{*l} and T_{*l} – Eqs. (7) and (6) respectively – using the following expression (Al-Jiboori, Xu & Qian, 2002):

$$\Lambda = \frac{u_{*l}^3 \overline{T}}{\kappa g \overline{w'T'}} \qquad (8)$$

where:
g – gravitational acceleration.

To obtain dimensionless local stability, it had been divided the height Z over Λ, i.e. Z / Λ. The stability values were classified to three ranges: unstable

($-Z / \Lambda > 0.1$), neutral $|\overline{+}0.1|$ and stable ($Z / \Lambda > 0.1$).

Under different stability conditions, the results of C_μ^2 (plotted on Y-axis) versus stability parameter (plotted on X-axis) for winter, spring and summer are presented. To decrease the scatter in C_μ^2 results, sometimes the logarithmic scale is used in some figures. In spite of lack data, in winter a liner relation is obvious with different slopes where more steep appears in summer. The behavior of data points can be followed by general linear regression:

$$C_\mu^2 = \alpha + \beta \cdot Z/\Lambda \qquad (9)$$

The values of constants α (intercept) and β (slope) based on experimental results were determined for each season and presented in Table 2.

TABLE 2. Value of constants α and β according to the three seasons

Season	Unstable		Neutral	Stable	
	α	β	α	α	β
Winter	72.0	72.9	12	–	–
Spring	202	112	163	0.6	0.4
Summer	1.6	0.8	7 181	3.3	2.0

Unstable conditions. The inverse direct relation of C_μ^2 with $- Z/\Lambda$ values for three seasons observed as illustrated in Figure 5. Across all figures, C_μ^2 results increase toward high values of instability with the correlation coefficient value 0.7. The values of instability are larger in summer than in winter and spring. This associates increasing turbulence intensity, but the turbulence is sometimes weak and the values decrease in the negative direction.
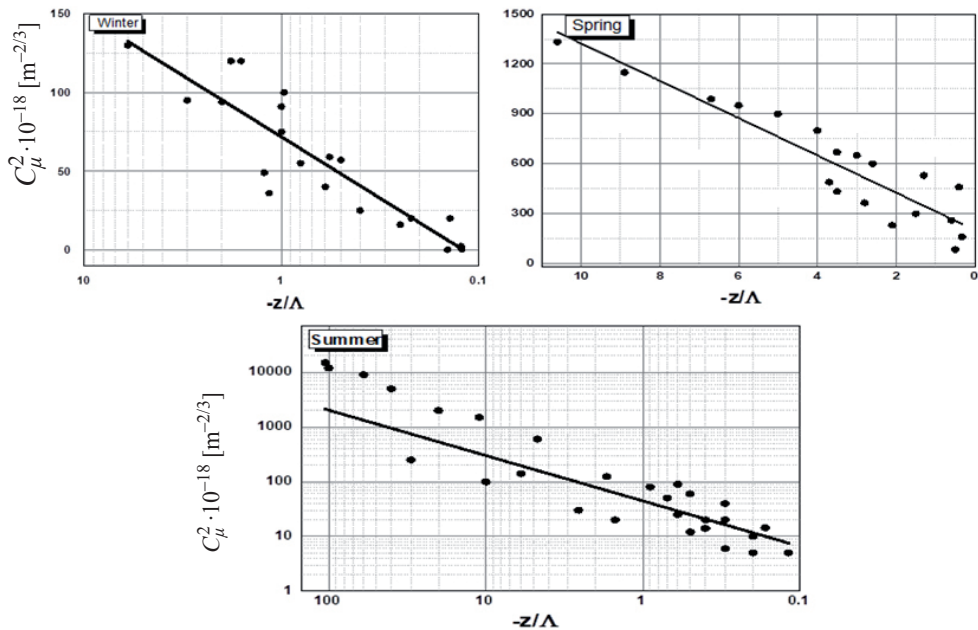
FIGURE 5. The effect of atmospheric stability under unstable conditions on C_μ^2 during three seasons

In spring season, since a visible phenomenon exists, this means that the turbulence exists but with less in winter and an increase with small magnitudes and we found that the values near zero and negative direction. During summer season, since the atmosphere is clear, this indicates that there is a high degree of instability because the turbulence is increasing during the sunny days.

When comparing air stability values for the three seasons of this work, they have large extent at summer relative to two remaining reasons. Of course, this come from high heat flux due to strong solar radiation as well as long summer days at Baghdad.

Neutral conditions. Neutral cases were determined as remaining after extracting unstable and stable cases and found few points that indicate the cases of equivalence. The values in general are between 0.08 and +0.1. There was no clear variation in C_μ^2 values over neutral segment, but seem to be roughly constants with values 12,163 and 7,181 m$^{-2/3}$ for winter, spring and summer, respectively (Table 1).

Stable conditions. The number of C_μ^2 data for stable conditions ($Z/\Lambda > 0$) were found to be less than that of unstable conditions, especially for both winter and spring, so they have more scattering as shown in Figure 6. In winter and spring, despite the values of C_μ^2 are small, they show a linear relation with increasing stability followed by Eq. (9) with values of constants α and β reported in Table 2. In other speech, turbulence is noted, but with weakness.

Since the thermal turbulence was fair in summer season, because the strong

heating resulting from the sun. The stability was taken off by spring season, and stability increases with increasing turbulence but by a small percentage and the reason for the emergence of stability is the existence of fog. As shown in Figure 6, there is a linear relationship and the stability was tilted to the positive direction. This behavior can be expressed by Eq. (9) with values of constants α and β reported in Table 2 for spring and summer seasons. The interesting feature here, the C_μ^2 values in spring and probably winter are very small compared to summer even under very stable condition. This may cause by frequency of weather situations such as rain, fog and clouds as shown in Table 1 and next sub-section.

In this sub section, the effect of atmospheric turbulence on C_μ^2 under rainy and foggy conditions are also studied.

Figure 7 shows the diurnal variation of rain and fog on C_μ^2. Unfortunately, just only three cases of rain are associated with the runs of this study, but they are provided a good indication about the behavior C_μ^2 under rain cases, whereas the C_μ^2 values sharply drop to the minimum even though at noon time. That means rain can eliminate thermal turbulence effect, especially at noon time. Fog formed can also decrease the C_μ^2 values to zero especially at night (Fig. 7), and then these values increase at day times where the fog starting disappears.

Figure 7 shows the extent of the effect of the rain, although the rain hours are few it can be verified that the value of C_μ^2 decreased almost to zero at 12:00 and 13:00. Under the fog condition, we notice that a low value of C_μ^2 starts from noon to 14:00 where it reaches almost
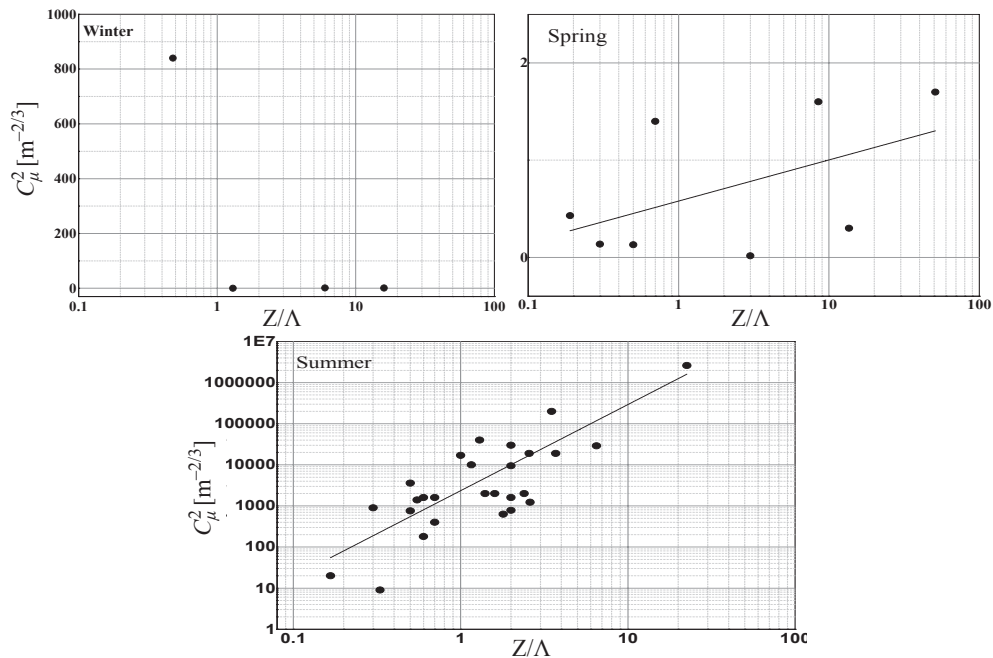

FIGURE 6. The effect of atmospheric stability under stable condotions on C_μ^2 during three seasons
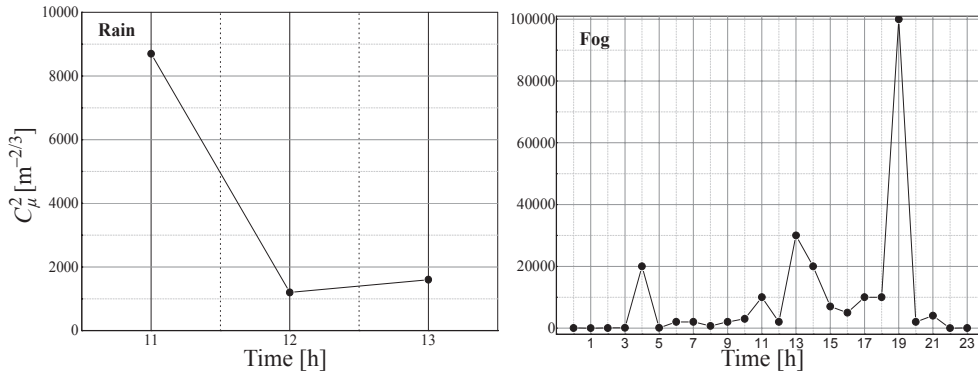
FIGURE 7. Effect of rain and fog on C_μ^2

zero, and fluctuated, but not much, and the highest value is at about 19:00 where the weather fog in this period is fogless.

From the discussion for the present paper above, the turbulence intensity effect on C_μ^2 increases at times from 9:00 to 14:00 where the turbulence was high during summer season, while decreasing this effect in winter and spring seasons. There were high fluctuations in the values of C_μ^2 between the sunrise and sunset periods of day, and they were eliminated at night. As for the winter season, the observed days represented the presence of rain. C_μ^2 results showed strong relation with stability where direct linear relation under stable, inverse under unstable and roughly constant under neutral conditions. Lastly, the C_μ^2 values dropped sharply to lowest at significant weather cases such as rain and fog.

References

Al-Jiboori, M.H., Xu, Y.M. & Qian, Y.F. (2002). Local similarity relationships in the urban boundary layer. *Boundary-Layer Meteorology*, *102*(1), 63-82.

Altowij, K.S., Alkholidi, A. & Habib, H. (2010). Effect of clear atmospheric turbulence on quality of free space optical communications in Yemen. *Frontiers of Optoelectronics in China, 3*(4), 423-428.

Beland, R.R. (1993). Propagation through atmospheric optical turbulence. *The infrared and electro-optical systems handbook* (pages 157-232). Bellingham, Washington' DC: MI and SPIE Engineering.

Canuet, L. (2014). *Atmospheric turbulence profile modeling for satellite-ground laser communication* (master thesis). Barcelona: Universitat Politêcnica de Catalunya [manuscript].

Fried, D.L. (1965). Statistics of a geometrical representation of wave front distortion. *Journal of the Optical Society of America, 55*, 1427--1435.

Hagelin, S., Masciadri, E. & Lascaux, F. (2005). Optical turbulence the influence of the atmosphere on ground–based astronomy. Earth Sciences. Uppsola: University.

Henniger, H. & Wilfert, O. (2010). An introduction to free-space optical communications. *Radioengineering*, *19*, 203-212.

Hulett, H.R. (1967). Turbulence limitation in photographic resolution of planet surfaces. *Journal of the Optical Society of America*, *57*, 1335-1338.

Ishimaru, A. (1997). *Wave propagation and scattering in random media*. New York: IEEE Press and Oxford University Press.

Panofsky, H. & Dutton, J. (1984). *Atmospheric turbulence: models and methods for engi-*

neering applications. Hoboken, NJ: John Wiley and Sons.

Prokeš, A. (2009). Modeling of atmospheric turbulence effecton terrestrial FSO link. *Radio Engineering*, *18*, 42-47.

Roadcap, J.R. & Tracy, P. (2009). A preliminary comparison of daylit and night C_μ^2 profiles measured by thermosonde. *Radio Science*, *44*. doi: 10.1029/2008RS00392

Romain, D., Larkin, M., Ghayel, G., Paulson, B. & Nykolak, G. (2001). Optical wireless propagation: theory vs. experiment. *Optical Wireless Communications III, Proc. SPIE, 4214*.

Walters, D.L., Kunket, K.E. & Hoidale, G.B. (1981). Diurnal and seasonal variations in the atmospheric structure parameter (C_μ^2) that affect the atmospheric modulation transfer function (MTF). *Atmospheric Transmission*, *277*, 6-9.

Wesely, M.L. & Alcaraz, E.C. (1973). Diurnal cycles of the refractive index structure function coefficient. *Journal of Geophysical Research*, *78*, 6224-6232.

Zhu, X.M. & Kahn, J.M. (2002). Free-space optical communication throughatmospheric turbulence channels. *IEEE Transactions on Communications*, *50*, 1293-1300.

Summary

Characteristics of C_μ^2 derived from ultrasonic anemometer in an urban boundary layer. Fast-response observations of three components of wind and air temperature have been applied to calculate the refractive index function coefficient (C_μ^2), which is needed to describe optical wave propagation in a turbulent medium. These were measured by 3D ultrasonic anemometer installed on the roof of the building of Atmospheric Science Department which is 19 m above ground level. Refractive index function coefficient was calculated for various periods of three seasons: winter, spring and summer.Diurnal variations of (C_μ^2) have been made at the surface layer for these seasons. The results show that high values ofmean (C_μ^2) occurred during the day time more than at night, also they occurred more in summer than in winter and spring. The results of (C_μ^2) found to change with atmospheric stability, whereas they inversely decrease under unstable conditions, approximately constant at neutral cases, and increase under stable conditions. Values of (C_μ^2) on average appears to be lower during the rainy and foggy weather cases compared to those of clear sky.

Authors address:
Monim H. Al-Jiboori, Sundus H. Jaber
Atmospheric Science Department
College of Science
Palestine Street, P.O. Box 14022
Mustansiriyah University, Baghdad
Iraq
e-mail: mhaljiboori@gmail.com
        Sundushassan91@gmail.com